Exosome-mediated radiosensitizing effect on neighboring cancer cells via reactive oxygen species production

Ai Nakaoka
Kobe Daigaku Daigakuin Igakukei Kenkyuka Igakubu
Makiko Nakahana
Kobe Daigaku Igakubu Fuzoku Byoin
Sachiko Inubushi
Kobe Daigaku Daigakuin Igakukei Kenkyuka Igakubu
Hiroaki Akasaka
Kobe Daigaku Daigakuin Igakukei Kenkyuka Igakubu
Mohammed Salah
Kobe Daigaku Daigakuin Igakukei Kenkyuka Igakubu
Hikaru Kubota
Kobe Daigaku Daigakuin Igakukei Kenkyuka Igakubu
Yoshiko Fujita
Kobe Daigaku Daigakuin Igakukei Kenkyuka Igakubu
Mennaallah Hassan
Kobe Daigaku Daigakuin Igakukei Kenkyuka Igakubu
Naritoshi Mukumoto
Kobe Daigaku Daigakuin Igakukei Kenkyuka Igakubu
Ryo Nishikawa
Kobe Daigaku Daigakuin Igakukei Kenkyuka Igakubu
Takeaki Ishihara
Kobe Daigaku Daigakuin Igakukei Kenkyuka Igakubu
Daisuke Miyawaki
Kobe Daigaku Igakubu Fuzoku Byoin
Kenji Yoshida
Kobe Daigaku Igakubu Fuzoku Byoin
Takashi Sasayama
Kobe Daigaku Daigakuin Igakukei Kenkyuka Igakubu
Ryohei Sasaki (rsasaki@med.kobe-u.ac.jp)
Division of Radiation Oncology, Kobe University Graduate School of Medicine https://orcid.org/0000-0002-4994-9386

Research

Keywords: Exosomes, cancer cells, reactive oxygen species, miRNA, DNA damage, intercellular communication, membrane vesicles, extracellular vesicles

Posted Date: March 12th, 2020

DOI: https://doi.org/10.21203/rs.3.rs-17026/v1

Abstract

Purpose/Objectives: The mechanism of intercellular communication after radiation exposure in cancer cells remains fully undetermined. Exosomes are lipid bilayer-constituted, membrane-enclosed small vesicles that are recognized as mediators transporting a variety of intracellular components including miRNA. Here we identified the novel role of exosomes released from irradiated cells to neighboring cancer cells.

Materials/Methods: Human pancreatic cancer cell line MIAPaCa-2 was used in this study. Purified exosome product (PEP) was obtained from cultured media by ultra-centrifugation. PEP was morphologically confirmed by transmission electron microscopy (TEM), and analyzed by NanoSight. Exosome-specific surface markers CD9 and CD63 were evaluated by western blotting. Endocytosis of irradiated exosomes was confirmed by fluorescent microscopy by using the PKH26 dye. Cell survival after irradiation was evaluated by a colony-forming assay. Intracellular reactive oxygen species (ROS) levels were determined using the oxidation-sensitive fluorescent probe dye C-H 2 DCF, and DNA damage was evaluated by detecting phosphorylated histone 2AX (γ-H2AX) foci by immunocytochemistry. MiRNAs were isolated from the exosomes after 5 Gy or 8 Gy of irradiation and comprehensive miRNA expression analysis was performed by miRNA microarray analyses. Expressions of Cu/Zn superoxide dismutase enzyme (SOD1) or Mn superoxide dismutase enzyme (SOD2), catalase, and glutathione peroxidase were studied to determine whether the exosomes received by the neighboring cells may have influence to them and lead to production of ROS or not.

Results: Exosome characteristics were confirmed by multiple methods. The uptake of irradiated exosomes was significantly higher than that of nonirradiated exosomes. Notably, nonirradiated neighboring cells with irradiated exosomes induced higher intracellular levels of ROS, and a higher frequency of DNA damage. These neighboring cells also showed greater sensitivity to radiation. Seven upregulated and 5 downregulated miRNAs were identified that correlated with the miRNA microarray analyses results obtained after 5 Gy and 8 Gy radiation. Among them, miR-6823-5p was identified as a possible candidate for SOD1 inhibition, leading to intracellular ROS production and DNA damage.

Conclusions : This is the first study to determine that irradiated exosomes can enhance the radiation effect via ROS production in cancer cells. This novel finding may lead to the understanding of the bystander effect of neighboring cancer cells.

Background

Exosomes are categorized as a membrane vesicle with a diameter of 30–100 nm, and constitute a subset of extracellular vesicles. As exosomes carry various bioactive molecules such as enzymes, cytokines, eicosanoids, and small RNAs, they play a critical role in intercellular communication [1]. Exosomes are unique in that they are formed and secreted by the cellular endosomal pathway. They are subsequently sorted based on different membrane-trafficking routes that involve the following activities: recycling of

exosomes back to the plasma membrane; formation of late endosomes followed by their degradation in lysosomes; and formation of late endosomes followed by their integration into exosomes in the multi-vesicular body [2]. Exosomes play a variety of critical roles in cancer progression, intercellular communication, tumor-stromal interactions, activation of signaling pathways, immunomodulation, and possibly some more crucial functions that are currently unknown [1, 3].

The level of reactive oxygen species (ROS) is increased in many types of cancer cells compared to normal cells [4]. A moderate increase in ROS levels can promote cell proliferation and differentiation [5], whereas high ROS levels can cause oxidative damage to lipids, proteins, and DNA. Therefore, maintaining ROS homeostasis is crucial. Cells maintain ROS homeostasis by balancing ROS generation with their elimination by antioxidant molecules such as superoxide dismutase (SOD). Radiotherapy potently induces massive cell death by triggering apoptosis in cancer cells via ROS generation [6]. During radiotherapy, ROS such as superoxide anions, hydroxyl radicals, and hydrogen peroxide (H_2O_2) molecules are generated by the radiolysis of water in the extracellular environment, and these highly reactive entities are toxic to both tumor cells and surrounding normal tissues [7].

MicroRNAs (miRNAs) are small noncoding RNAs composed of 18–22 nucleotide sequences that perform a regulatory role by binding to their target mRNAs via multiple imperfect base pairings within the 3'-untranslated region (3'-UTR). MiRNAs have a wide range of targets that allow them to modulate many pathways involved in cancer progression including cell proliferation, apoptosis, metastasis, and angiogenesis [8]. They are differentially expressed in normal and cancer cells, and some miRNAs may act as tumor suppressors while others as oncogenes, thus promoting tumor initiation and progression [9]. MiRNA expression is altered in both radiation-exposed cancer cells [10–12] and normal cells [13–14], and its expression profile is modulated in response to DNA damage [15–16]. However, whether these altered miRNAs may contribute to intercellular communication and may be delivered to recipient cells via exosomes remain unclear.

Irradiated cells can generate communication signals and subsequently cause biological changes in neighboring or distant nonirradiated cells, and this phenomenon is called radiation-induced bystander effect (RIBE). A variety of signaling molecules such as ROS [17], cytokines [18–19], and exosomes [20] are initiators of such bystander responses. However, the role of exosome in RIBE, and the relationship between ROS and exosomes remain largely uncertain.

In this study, we intensively evaluated the role of exosomes in radiation response using the human pancreatic cancer cell line MIAPaCa-2. Notably, exosomes released after radiation enhanced the radiation effect but did not cause radioresistance. Here we introduce the molecular events mediated by exosomes in RIBE via ROS production.

Materials And Methods

Cells culture and reagents

The MIAPaCa-2 human pancreatic cancer cell line was obtained from Japanese Collection of Research Bioresources Cell Bank (JCRB) and maintained in minimal essential medium (MEM) medium containing 10% exosome-free fetal bovine serum (FBS) and nonessential amino acids at 37°C in 5% CO_2. The following antibodies were purchased: anti-cytochrome C and anti-Phosphorylated histone H2AX (γ-H2AX) from Cell Signaling Technology Inc. (Danvers, MA, USA), anti-CD9, anti-catalase (Cat), and anti-glutathione peroxidase 1 (GPx1) from Abcam (UK); anti-CD63 from Medical and Biological Laboratories (MBL, Nagoya, Japan); and anti-actin from Santa Cruz Biotechnology, Inc., (Dallas, TX, USA); anti-SOD1 and anti-SOD2 from Merck (Darmstadt, Germany); and tetramethyl rhodamine isothiocyanate (TRITC)-conjugated anti-rabbit secondary antibody from Agilent Technology (Tokyo, Japan). The following reagents were purchased: PKH-26, a lipophilic dye, and N-acetyl-L-cysteine (NAC) from Sigma-Aldrich Co. (St. Louis, MO, USA); Hoechst 33342 (Hoechst) and 2′,7′-dichlorodihydrofluorescein diacetate (C-H_2DCF) from Thermo Fisher Diagnostics K.K. (Tokyo, Japan); Methylene Blue from Wako (Osaka, Japan); and 4′,6-diaidino-2-phenylindole (DAPI) from Agilent Technology.

Isolation and morphological evaluation of exosomes

Exosomes were isolated from media-conditioned cells by ultracentrifugation [21]. Briefly, MIAPaCa-2 cells were seeded at 2.0 × 10^6 cells per T75 cm^2 flask and irradiated after substituting the media with exosome-depleted 10% FBS cell culture media. The cell culture media was centrifuged at 2,000 ×g for 10 min at 4°C, and the supernatants were filtered through a 0.22 μm minisart syringe filter (Sartorius, Goettingen, Germany). The supernatants were ultracentrifuged at 150,000 ×g for 90 min at 4°C. The pellet was washed with phosphate-buffered saline (PBS) and ultracentrifuged at 150,000 ×g for 90 min at 4°C and resuspended in 50 μL PBS.

The exosomes isolated from nonirradiated cells (0 Gy-Exo) and those isolated from 5 Gy irradiated cells (5 Gy-Exo) were evaluated by transmission electron microscopy (TEM). Briefly, 4 mL of the PBS suspension of isolated exosomes was loaded onto carbon-coated 200 mesh copper grids for 1 min at room temperature. Excessive fluid was slightly drained using filter papers. The adsorbed exosomes were negatively stained with 2% uranyl acetate for 30 seconds. Finally, the air-dried exosome-containing grids were observed under TEM (JEM-1400plus, Japan) operating at 120 kV. Exosome size, concentration, and distribution were analyzed by nanoparticle tracking analysis (NTA) software using NanoSight NS300 (Malvern, Kobe, Japan). The software was optimized to first identify and then track each particle on a frame-by-frame basis, and its Brownian movement was tracked and measured from frame to frame (See Additional file 1).

Labelling of exosomes

Exosomes were labeled with the fluorescent dye PKH-26 using the PKH-26 labeling kit (Sigma-Aldrich Co.) [22]. Briefly, 0 Gy-Exo and 5 Gy-Exo were labeled with 2 μM PKH-26 for 15 min at room temperature. Thereafter, free PKH-26 was removed by ultrafiltration using the VIVACON 500 ultracentrifugation device (100,000 MWCO; Sartorius Stedim Biotech GmbH, Goettingen, Germany). The labeled exosomes were added to MIAPaCa-2 cell samples and the nuclei of cells were stained with Hoechst 33342 for 5 min.

Irradiation

Cells were exposed to a 5 Gy or 8 Gy dose of X-rays delivered at 0.57 Gy/min from an MBR-1505R2 generator (Hitachi Medical Corporation, Tokyo, Japan). The beam was filtered through a 1-mm aluminum board [23].

Colony-forming assay

Cell survival after irradiation was evaluated by performing a colony-forming assay with or without 5 Gy-Exo. Cells were reseeded into 6-well cell culture plates (Corning. Co., Tokyo, Japan) at a density of 200–4000 cells/well and incubated for 7 days. At the end of each experiment with 0 Gy-Exo, or with 5 Gy-Exo, the cells were fixed with a solution of 10% methanol and 20% acetic acid for 30 min, and stained with Methylene Blue for 30 min [24]. Colonies with ≥ 50 cells were counted. The experiment was performed in duplicates and repeated at least twice.

Determining intracellular ROS levels

Intracellular ROS levels were determined using the oxidation-sensitive fluorescent probe dye C-H_2DCF. Cells were seeded in 6-well plates (1.5×10^5 cells/well) overnight and treated with 5 Gy of radiation with or without 10 mg/mL 5 Gy-Exo and 1 mM NAC for 24 h [25]. After washing twice with FBS-free media, the cells were stained with 50 mM C-H_2DCF for 1 h at 37°C. Then, the nuclei of cells were stained with Hoechst 33342 for 5 min. The fluorescence of C-H_2DCF was visualized by using a fluorescence microscope (BZ-9000, Keyence, Osaka, Japan).

Detection of DNA damage after exosome uptake

Induction of DNA damage was investigated by detecting phosphorylated histone 2AX (γ-H2AX) foci using immunocytochemistry as described previously [26]. Cells were subcultured on 35-mm dishes, and treated with 10 mg/mL 5 Gy-Exo and 1 mM NAC for 24 h and/or 5 Gy of irradiation. Thereafter, the cells were fixed in 4% paraformaldehyde in PBS for 20 min, permeabilized with 0.1% Triton X-100 in PBS for 5 min,

and blocked in 5% bovine serum albumin in PBS for 60 min. The cells were incubated with 1:200 rabbit anti γ-H2AX antibody overnight at 4°C. Then, the cells were incubated with 1:20 TRITC-conjugated secondary antibody for 90 min at room temperature. The nuclei were stained with DAPI. The stained cells were observed using a fluorescence microscope. The cells expressing nuclear γ-H2AX foci were then counted manually from 100 cells for each treatment [27].

Immunoblotting

The expression levels of CD9, CD67, and cytochrome C were analyzed by western blotting. Briefly, 3 g of exosome or 30 g whole cell lysates were loaded onto 12% gels. After electrophoresis (30 mA), the proteins were transferred onto polyvinylidene difluoride membranes that were blocked with 5% nonfat milk and then incubated with primary antibodies. After washing, the membrane was incubated with horseradish peroxidase conjugated anti-CD9 or anti-CD63, and the expression levels were detected under nonreducing conditions. The expression levels of SOD1, SOD2, catalase, and glutathione peroxidase 1 were analyzed by western blotting. Briefly, the cells were seeded at 1.0×10^5 cells per T25 cm^2 flask and subject to 8 Gy radiation or 8 Gy-Exo was added (30 mg). Each protein was collected 24 h after these treatments. The intensity of each signal was analyzed by using Image J software and then, the ratios of SOD1, SOD2 catalase, glutathione peroxidase, and actin levels were calculated.

Total RNA extraction from exosomes and miRNA microarray analysis

Toray's 3D-Gene RNA-extraction reagent from a liquid sample kit was used (Toray Industries, Inc.). Comprehensive miRNA expression analysis was performed using a 3D-Gene miRNA Labeling Kit and a 3D-Gene Human miRNA Oligo Chip Ver. 21 (Toray Industries, Inc.) according to the manufacturer's protocol that was designed to detect 2565 human miRNA sequences. The expression level of each miRNA was expressed as the background-subtracted signal intensity of all the miRNAs in each microarray. Any signal intensity in both the duplicate spots at >1.5 standard deviation (SD) of the background signal intensity was considered a valid measurement.

Database processing analyses and miRNA identification

MiRNAs from exosomes isolated from cells either after 5 Gy or 8 Gy of radiation were visualized in the form of a heat map generated using the R software (version 3.5.3) and heatmap.2 from the gplots package (version 3.0.1.1). The analysis was performed by using the miRNAs whose ratios of expression levels between control and 5 Gy-Exo or 8 Gy-Exo were <0.5 or >1.5. The expression of miRNAs was normalized and then converted $\log_e$ values. In addition, we searched the targets of these miRNAs that

caused ROS production from the databases using TargetScan and miRTarBase. MiRNAs were then clustered using hierarchical clustering with Euclidean distance and complete linkage.

Results

Characterization of exosomes

The purity, quality, and morphology of the exosomes were analyzed. The isolated exosomes were shaped in the form of closed, round vesicles with a diameter of approximately 100 nm. The morphological features of 0 Gy-Exo and 5 Gy-Exo were similar according to TEM observations (Fig. 1A). Each distribution profile for 0 Gy-Exo and 5 Gy-Exo revealed a peak of 107 nm and 101 nm by NanoSight, respectively (Fig. 1B). CD9 and CD63 expression was observed in both whole cell lysate and exosomes, while cytochrome C expression was detected only in the whole cell lysate (Fig. 1C). These data indicated that the exosomes were successfully isolated from the culture media supernatants without contamination due to cellular components.

Cellular uptake of exosomes and survival

The uptake of 5 Gy-Exo increased compared to that of 0 Gy-Exo (Fig. 2A). Cells were irradiated and treated with or without 5 Gy-Exo (Fig. 2B). As a result, the cells irradiated with 5 Gy-Exo showed an increased radiosensitizing effect in an exosome concentration-dependent manner (Fig. 2C).

Exosomes increased intercellular ROS levels

ROS production was evaluated by using C-H_2DCF. Interestingly, intercellular ROS levels increased by adding 5 Gy-Exo (Exosome) and by 5 Gy of radiation (IR), and those increased greater by the combination of 5 Gy and 5 Gy-Exo (IR + Exo). Those intercellular ROS significantly decreased by adding the ROS scavenger, NAC (IR + Exo + NAC) (Fig. 3A and 3B).

DNA damage after exosome uptake

Notably, 5 Gy-Exo increased the number of γH2AX-positive cells with the same dose of radiation, and a combination 5 Gy-Exo and 5 Gy of radiation led to a significantly greater number of γH2AX-positive cells. Cell stained with NAC produced lesser γH2AX signals, indicating that DNA damage was induced by ROS production (Fig. 4A and 4B).

Identification of miRNA in exosomes after radiation

Seven upregulated and 5 downregulated miRNAs were identified that were consistent with the results obtained after 5 Gy and 8 Gy radiation (Fig. 5A), and stratified by a heat map (Fig. 5B). The possible targets of the miRNAs that may be associated with ROS production were identified from the databases using TargetScan and miRTarBase. Based on our search results, miR-6823-5p was identified as a

possible candidate for SOD1 inhibition, and subsequent analysis proved the inhibitory effect of miR-6823-5p.

Exosomes inhibited the expression of SOD1 in cancer cells

Cells were treated with 5 Gy of radiation or 5 Gy-Exo, after which the expression levels antioxidant enzymes including SOD1, SOD2, catalase, and glutathione peroxidase were analyzed. The SOD1 expression was decreased by adding 5 Gy-Exo, while those of SOD2 catalase, or glutathione peroxidase were not (Fig. 6A). The part of complementary sequence site of SOD1 was corresponding with miR-6823-5p (Fig. 6B). These results suggested that miR-6823-5p in the exosomes derived from irradiated cells may contribute to a decrease in SOD1 expression.

Discussion

The main focus of this study was to prove that irradiated exosomes induced ROS production in neighboring cancer cells leading to the amplification of the radiation effect. The possible mechanisms of this finding seem to be the transportation of certain miRNAs via irradiated exosomes. To best of our knowledge, this is first study to report that *miR-6823-5p* was identified as the candidate for causing the inhibition of SOD1 expression in response to radiation.

SOD1 is overexpressed in several cancer cells and that the activity of SOD1 may be essential to maintain cellular ROS level. Papa L. et al. [28] reported that there are SOD1 plays an important role in cancer progression, and the potential cross-talk between SOD1 overexpression and regulation of the mitochondrial unfolded-protein response UPRmt. Cells must continuously cope with extensive intracellular oxidative stress generated by ROS and reactive nitrogen species (RNS). To control the genotoxic effects of ROS/RNS and to exploit them in diverse functions including signaling, cells regulate their levels with the help of various antioxidants including SODs. Gomes S et al. [29] demonstrated that the expression of SOD1 was reduced in cells overexpressing *miR-143* or *miR-145* using the HCT116 colon cancer cell line. Furthermore, *miR-143* overexpression increased ROS generation, which was abrogated by the reintroduction of SOD1. In our study, *miR-143* or *miR-145* did not increase in exosomes in the MIAPaCa-2 human pancreatic cancer cell line. The possible explanation of this difference might be that our results were derived from responsive miRNAs in exosomes obtained after radiation exposure. Other possible reasons might be the different sources of miRNAs. The results of the previous study were obtained using a cancer cell line, while ours was obtained used exosomes.

Inhibition of SOD1 expression by exosomes has not been reported previously. Furthermore, there are no studies reporting that exosomes from irradiated cells induced DNA damage via ROS production. Thus, our findings seem important for investigating exosome functions in response to radiation. Glasauer A et al. [30] showed that inhibition of SOD1 expression either by small hairpin RNA (shRNA) or an SOD1 inhibitor named ATN-224 drastically reduces the ability of the lung carcinoma cell line A549 to form colonies on soft agar. They further reported the unexpected finding that inhibition of SOD1 expression

leads to an increase rather than a decrease in H_2O_2 levels, which resulted from the inhibition of the glutathione peroxidase enzymes by superoxide, suggesting that the inhibition of SOD1 induces cell death by apoptosis [30]. Taken together, SOD1 modulation seems to be a promising target for enhancing the radiation effect.

Our findings might be one of the novel mechanisms that could explain RIBE, which has been observed in a variety of endpoints including DNA damage induction [31], induction of mutations [32-33], cell death or apoptosis [34], altered gene expression [8, 19], and alteration in the miRNA profile [35-36]. Ionizing radiation (IR) is frequently accompanied by marked changes in the miRNA profile of cells. Although miRNAs have also been implicated in ROS level regulation through the regulation of enzymes involved in ROS metabolism [37], the relationship between exogenous ROS and intercellular communication via exosomes has not been elucidated. ROS production has been implicated in mediating radiotherapy responses due to DNA damage on downstream cell survival or death signaling cascades [38-39]. Cancer cell-derived exosomes have been demonstrated to play a role in promoting cancer cell invasiveness and metastasis, and activation of relevant oncogenic pathways [40-41].

The effect exosomes obtained from irradiated cancer cells on recipient cells is also another interesting aspect. We also studied intercellular communication between cancer cells via exosomes that included communication between cancer cells, and between cancer cells and stromal, vascular, and immune cells. Cancer cell-secreted exosomes affect either other cancer cells or host cells, and may lead to the secretion of more exosomes than nonmalignant cells. The process by which recipient cells take up exosomes is still not well understood, and whether exosomes even need to be taken up to execute a cellular response remains unclear. A growing body of evidence indicates that exosomes mediate the delivery of proteins, mRNAs, and miRNAs from cancer cells to recipient or neighboring cells by intercellular communication, which may assist in the creation of a metastatic niche and facilitate cancer cell progression and metastasis, or influence the activity and/or behaviors of recipient cells [42-43]. The results of SOD1 inhibition obtained from this study may be investigated in further study as a new role of irradiated exosomes.

In conclusion, this is the first study to identify a novel function of irradiated exosome in terms of their ability to enhance the radiation effect via ROS production in cancer cells. This finding may lead to the understanding of bystander effect between neighboring cancer cells.

Abbreviations

miRNA, microRNA

RNA, ribonucleic acids

PEP, Purified exosome product

TEM, transmission electron microscope

ROS, reactive oxygen species

C-H_2DCF, 2′,7′-dichlorodihydrofluorescein diacetate

DNA, deoxyribonucleic acid

γ-H2AX, phosphorylated histone 2AX

SOD1, Cu/Zn superoxide dismutase enzyme

SOD2, Mn-superoxide dismutase enzyme

SOD, superoxide dismutase

H_2O_2, hydrogen peroxide

3′-UTR, 3'-untranslated region

RIBE, radiation induced bystander effect

MEM, minimal essential medium

FBS, Fetal bovine serum

TRITC, Tetramethyl rhodamine isothiocyanate

NAC, N-acetyl-L-cysteine

Hoechst, Hoechst 33342

DAPI, 4', 6-diaidino-2-phenylindole

PBS, phosphate buffered saline

NTA, nanoparticle tracking analysis

SD, standard deviationGPX-1, Glutathione Peroxidase1

UPRmt, mitochondrial unfolded-protein response

RNS, reactive nitrogen species

shRNA, small hairpin RNA

GPX, Glutathione Peroxidase

mRNA, messenger RNA

Declarations

Conflict of interest: None.

Ethics approval and consent to participate: Not applicable.

Acknowledgment: We thank Prof. Nitta and Dr. Imasaki of division of Structural Medicine and Anatomy, Kobe University Graduate School of Medicine for their helpful advices.

Funding: This work was supported by Grants-in-Aid for Exploratory Research [grant numbers18K07752 to Hideki Nishimura and RS; 19K08097 to Aya Harada and RS, 08K07676 to SI and RS] from the Ministry of Education, Culture, Sports, Science, and Technology of Japan. Parts of the data were presented at the 7th Japan-Taiwan Radiation Oncology symposium, Tokyo, Japan, May 11, 2019.

Author contribution:

AN, SI, HA, and RS: conception and design of the study;

AN, MN, MS, YF, MH, NM, RN, TI, DM, TS, and RS: acquisition, analysis, and interpretation of data;

AN, HK, KY, and RS: drafting and critically revising the manuscript for important intellectual content.

All authors approved the final version of the manuscript.

Author information:

Ai Nakaoka, Email: ai21kitune47@gmail.com

Makiko Nakahana, Email: nakahana-m@people.kobe-u.ac.jp

Sachiko Inubushi, Email: sachiko_inubushi@people.kobe-u.ac.jp

Hiroaki Akasaka, Email: akasaka@harbor.kobe-u.ac.jp

Mohammed Salah, Email: drsalahbio@yahoo.com

Hikaru Kubota, Email: hk0113hu@med.kobe-u.ac.jp

Yoshiko Fujita, Email: cafe445@gmail.com

Mennaallah Hassan, Email: menna_alesawy@ymail.com

Naritoshi Mukumoto, Email: nmukumot@med.kobe-u.ac.jp

Ryo Nishikawa, Email: rnskw@med.kobe-u.ac.jp

Takeaki Ishihara, Email: take3036@med.kobe-u.ac.jp

Daisuke Miyawaki, Email: miyawaki@med.kobe-u.ac.jp

Kenji Yoshida, Email: kyoshi@med.kobe-u.ac.jp

Takashi Sasayama, Email: takasasa@med.kobe-u.ac.jp

Ryohei Sasaki, Email: rsasaki@med.kobe-u.ac.jp

References

1. Tkach M, Théry C. Communication by extracellular vesicles: where we are and where we need to go. Cell. 2016;164:1226-32.
2. Hessvik NP, Llorente A. Current knowledge on exosome biogenesis and release. Cell Mol Life Sci. 2018;75:193-208.
3. Greening DW, Gopal, SK, Xu R, Simpson RJ, Chen W. Exosomes and their roles in immune regulation and cancer. Semin Cell Dev Biol. 2015;40:72-81.
4. Szatrowski TP, Nathan CF. Production of large amounts of hydrogen peroxide by human tumor cells. Cancer Res. 1991;51:794-8.
5. Boonstra J, and Post JA. Molecular events associated with reactive oxygen species and cell cycle progression in mammalian cells. Gene. 2004;337:1-13.
6. Srinivas US, Tan B WQ, Vellayappan BA, Jeyasekharan AD. ROS and the DNA damage response in cancer. Redox Biol. 2019;25:101084.
7. Zou Z, Chang H, Li H, Wang S. Induction of reactive oxygen species: An emerging approach for cancer therapy. Apoptosis. 2017;22:1321-35.
8. Shea A, Harish V, Afzal Z, Chijioke J, Kedir H, Dusmatova S, et al. MicroRNAs in glioblastoma multiforme pathogenesis and therapeutics. Cancer Med. 2016;5:1917-46.
9. Bracken CP, Scott HS, Goodall GJ. A network-biology perspective of microRNA function and dysfunction in cancer. Nat Rev Genet. 2016;17(12):719-32.
10. Di Francesco A, De Pittà C, Moret F, Barbieri V, Celotti L, Mognato M. The DNA-damage response to γ-radiation is affected by miR-27a in A549 cells. Int J Mol Sci. 2013;14(9):17881-96.
11. Zhang B, Chen J, Ren Z, Chen Y, Li J, Miao X, et al. A specific miRNA signature promotes radioresistance of human cervical cancer cells. Cancer Cell Int. 2013;13(1):118.
12. Shin S, Cha HJ, Lee EM, Lee SJ, Seo SK, Jin HO, et al. Alteration of miRNA profiles by ionizing radiation in A549 human non-small cell lung cancer cells. Int J Oncol. 2009;35(1):81-6.
13. Simone BA, Ly D, Savage JE, Hewitt SM, Dan TD, Ylaya K, et al. microRNA alterations driving acute and late stages of radiation-induced fibrosis in a murine skin model. Int J Radiat Oncol Biol Phys.

2014;90(1):44-52.
14. Hou J, Wang F, Kong P, Yu PK, Wang H, Han W. Gene profiling characteristics of radioadaptive response in AG01522 normal human fibroblasts. PLoS One. 2015;10(4):e0123316.
15. Sharma V, Misteli T. Non-coding RNAs in DNA damage and repair. FEBS Lett. 2013;587:1832-9.
16. Zhang C, Peng G. Non-coding RNAs: An emerging player in DNA damage response. Mutat Res. 2015;763:202-11.
17. Lyng FM, Maguire P, McClean B, Seymour C, Mothersill C. The involvement of calcium and MAP kinase signaling pathways in the production of radiation-induced bystander effects. Radiat Res. 2006;165(4):400-9.
18. Iyer R, Lehnert BE, Svensson R. Factors underlying the cell growth-related bystander responses to alpha particles. Cancer Res. 2000;60(5):1290-8.
19. Gow MD, Seymour CB, Ryan LA, Mothersill CE. Induction of bystander response in human glioma cells using high-energy electrons: a role for TGF-beta1. Radiat Res. 2010;173(6):769-78.
20. Al-Mayah AHJ, Irons SL, Pink RC, Carter DRF, Kadhim MA. Possible role of exosomes containing RNA in mediating nontargeted effect of ionizing radiation. Radiat Res. 2012;177(5):539-45.
21. Thery C, Amigorena S, Raposo G, Clayton A. Isolation and characterization of exosomes from cell culture supernatants and biological fluids. In Current Protocols Cell Biology. 2006, Chapter 3:Unit 3.22.
22. Pegtel DM, Cosmopoulos K, Thorley-Lawson DA, van Eijndhoven MA, Hopmans ES, et al. Functional delivery of viral miRNAs via exosomes. Proc Natl Acad Sci USA. 2010;107:6328-33.
23. Shimizu Y, Mukumoto N, Idrus N, Akasaka H, Inubushi S, Yoshida K, et al. Amelioration of radiation enteropathy by dietary supplementation with reduced coenzyme Q10. Adv Radiat Oncol. 2019;4(2):237-45.
24. Achanta G, Sasaki R, Feng L, Carew JS, Lu W, Pelicano H, et al. Novel role of p53 in maintaining mitochondrial genetic stability through interaction with DNA Pol gamma. EMBO J. 2005;24(19):3482-92.
25. Sasaki R, Suzuki Y, Yonezawa Y, Ota Y, Okamoto Y, Demizu Y, et al. DNA polymerase gamma inhibition by vitamin K3 induces mitochondria-mediated cytotoxicity in human cancer cells. Cancer Sci. 2008;99(5):1040-8.
26. Nakayama M, Sasaki R, Ogino C, Tanaka T, Morita K, Umetsu M, et al. Titanium peroxide nanoparticles enhanced cytotoxic effects of X-ray irradiation against pancreatic cancer model through reactive oxygen species generation in vitro and in vivo. Radiat Oncol. 2016;11(1):91.
27. Bonner WM, Redoc CE, Dickey JS, Nakamura AJ, Sedelnikova OA, Solier S, et al. γH2AX and cancer. Nat Rev Cancer. 2008;8:957-67.
28. Papa L, Manfredi G, Germain D. SOD1, an unexpected novel target for cancer therapy. Genes Cancer. 2014;5(1-2):15-21.

29. Gomes SE, Pereira DM, Roma-Rodrigues C, Fernandes AR, Borralho PM, Rodrigues CMP. Convergence of miR-143 overexpression, oxidative stress and cell death in HCT116 human colon cancer cells. PLoS One. 2018;13(1):e0191607.
30. Glasauer A, Sena LA, Diebold LP, Mazar AP, Chandel NS. Targeting SOD1 reduces experimental non-small-cell lung cancer. J Clin Invest. 2013;124(1):117-28.
31. Yang H, Assad N, Held KD. Medium-mediated intercellular communication is involved in bystander responses of X-ray-irradiated normal human fibroblasts. Oncogene. 2005;24:2096-103.
32. Zhou H, Randers-Pehrson G, Waldren CA, Vannais D, Hall EJ, Hei TH. Induction of a bystander mutagenic effect of alpha particles in mammalian cells. Proc Natl Acad. Sci USA. 2000;97:2099-104.
33. Huo L, Nagasawa H, Little JB. HPRT mutants induced in bystander cells by very low fluences of alpha particles result primarily from point mutations. Radiat Res. 2001;156:521-5.
34. Lyng FM, Seymour CB, Mothersill C. Initiation of apoptosis in cells exposed to medium from the progeny of irradiated cells: a possible mechanism for bystander-induced genomic instability? Radiat Res. 2002;157:365-70.
35. Kovalchuk O, Zemp FJ, Filkowski JN, Altamirano AM, Dickey JS, Jenkins-Baker G, et al. MicroRNAome changes in bystander three-dimensional human tissue models suggest priming of apoptotic pathways. Carcinogenesis. 2010;31:1882-8.
36. Koturbash I, Zemp F, Kolb B, Kovalchuk O. Sex-specific radiation-induced microRNAome responses in the hippocampus, cerebellum and frontal cortex in a mouse model. Mutat Res. 2011;722(2):114-8.
37. Zhang X, Ng WL, Wang P, Tian L, Werner E, Wang H, et al. MicroRNA-21 modulates the levels of reactive oxygen species by targeting SOD3 and TNFa. Cancer Res. 2012;72:4707-13.
38. Fan PC, Zhang Y, Wang Y, Wei W, Zhou YX, Xie Y, et al. Quantitative proteomics reveals mitochondrial respiratory chain as a dominant target for carbon ion radiation: delayed reactive oxygen species generation caused DNA damage. Free Radic Biol Med. 2019;130:436-45.
39. Zulato E, Ciccarese F, Agnusdei V, Pinazza M, Nardo G, Iorio E, et al. LKB1 loss is associated with glutathione deficiency under oxidative stress and sensitivity of cancer cells to cytotoxic drugs and gamma-irradiation. Biochem Pharmacol. 2018;156:479-90.
40. Urbanelli L, Magini A, Buratta S, Brozzi A, Sagini K, Polchi A. Signaling pathways in exosomes biogenesis, secretion and fate. *Genes.* 2013;4:152-70.
41. Cardiello C, Cavallini L, Spinelli C, Yang J, Reis-Sobreiro M, de Candia P, et al. Focus on extracellular vesicles: new frontiers of cell-to-cell communication in cancer. *Int J Mol Sci.* 2016;17:175
42. O'Brien K, Rani S, Corcoran C, Wallace R, Hughes L, Friel AM, et al. Exosomes from triple-negative breast cancer cells can transfer phenotypic traits representing their cells of origin to secondary cells. *Eur J Cancer.* 2013;49:1845-59.
43. Costa-Silva B., Aiello NM, Ocean AJ, Singh S, Zhang H, Thakur BK, et al. Pancreatic cancer exosomes initiate pre-metastatic niche formation in the liver. *Nat Cell Biol.* 2015;17:816-26.

Figures

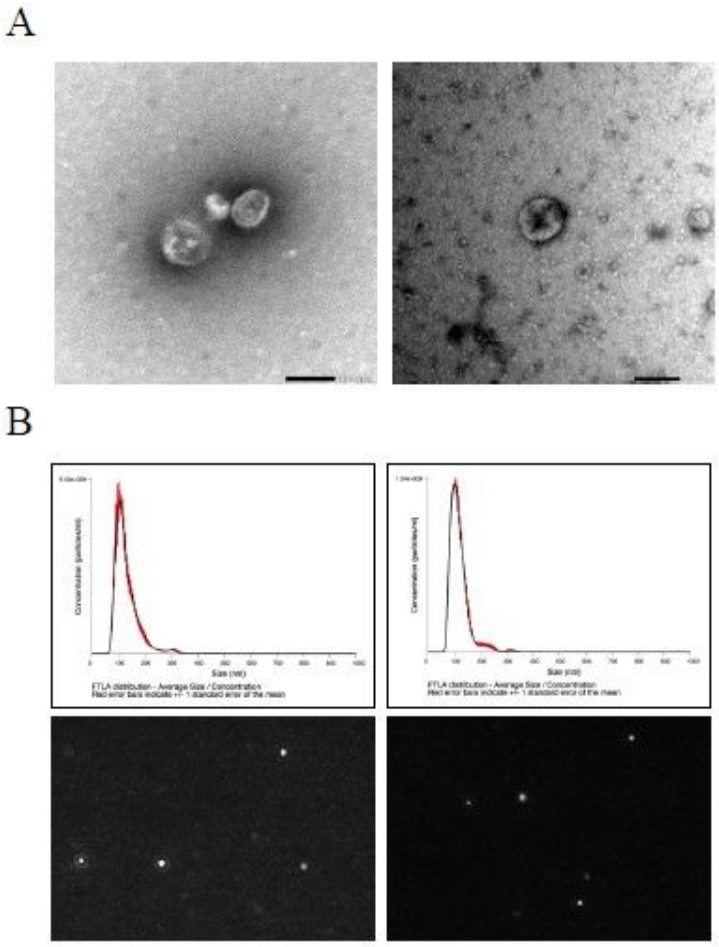

Figure 1

Typical features and characteristics of an exosome. A) TEM images. Scale bar indicates 100 nm. B) Size distribution illustrated by Nanosight. C) Western blotting of exosome markers (CD9 and CD63) and whole cell marker (cytochrome C).

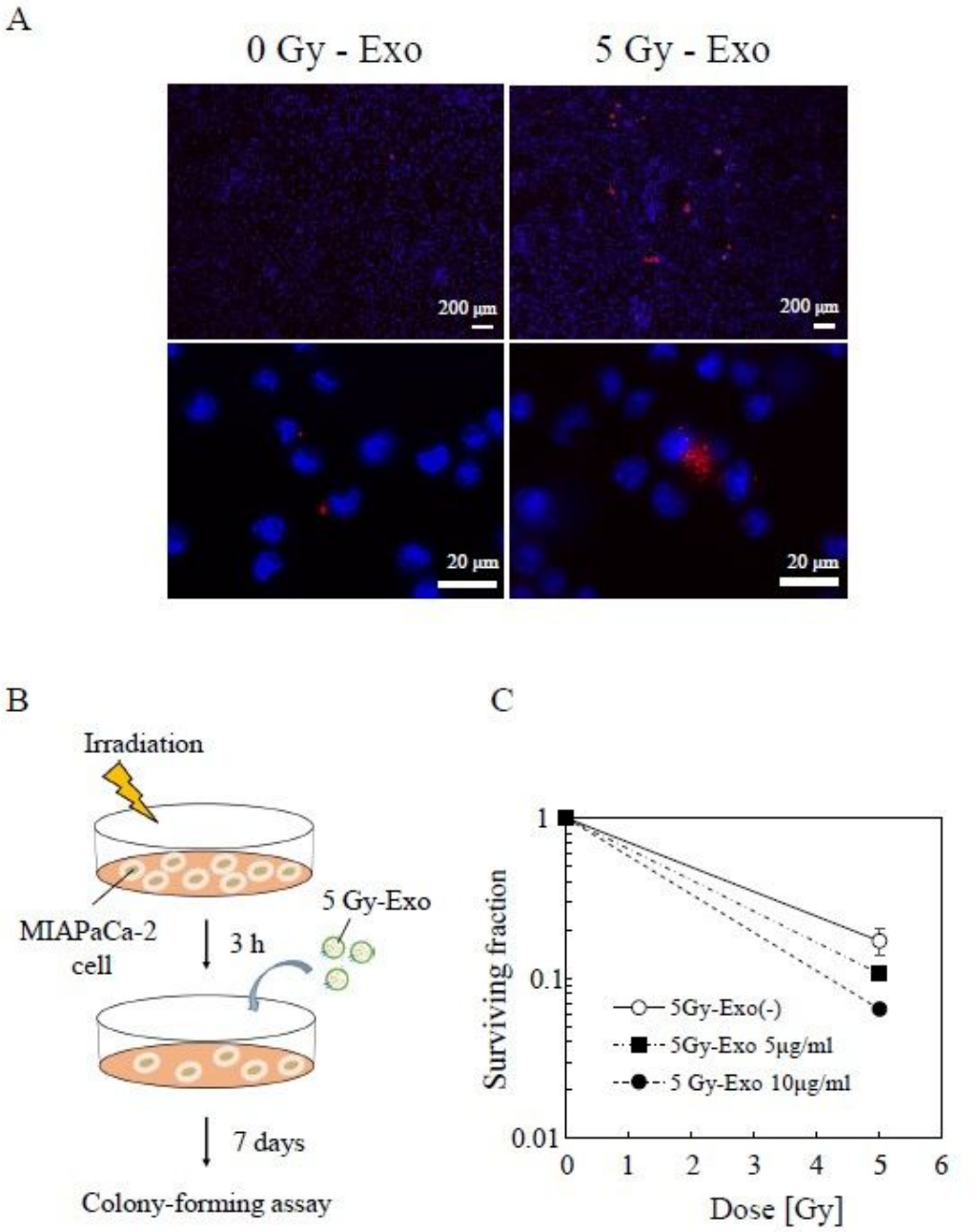

Figure 2

A) Representative images showing exosome uptake. 5 Gy-Exo (red) was more frequently observed in cells counterstained with Hoechst (blue). B) Schema of colony forming assay after adding the exosomes. C)

Surviving fractions. Values represent mean ± SE. P-value was calculated by using Student's t-test.

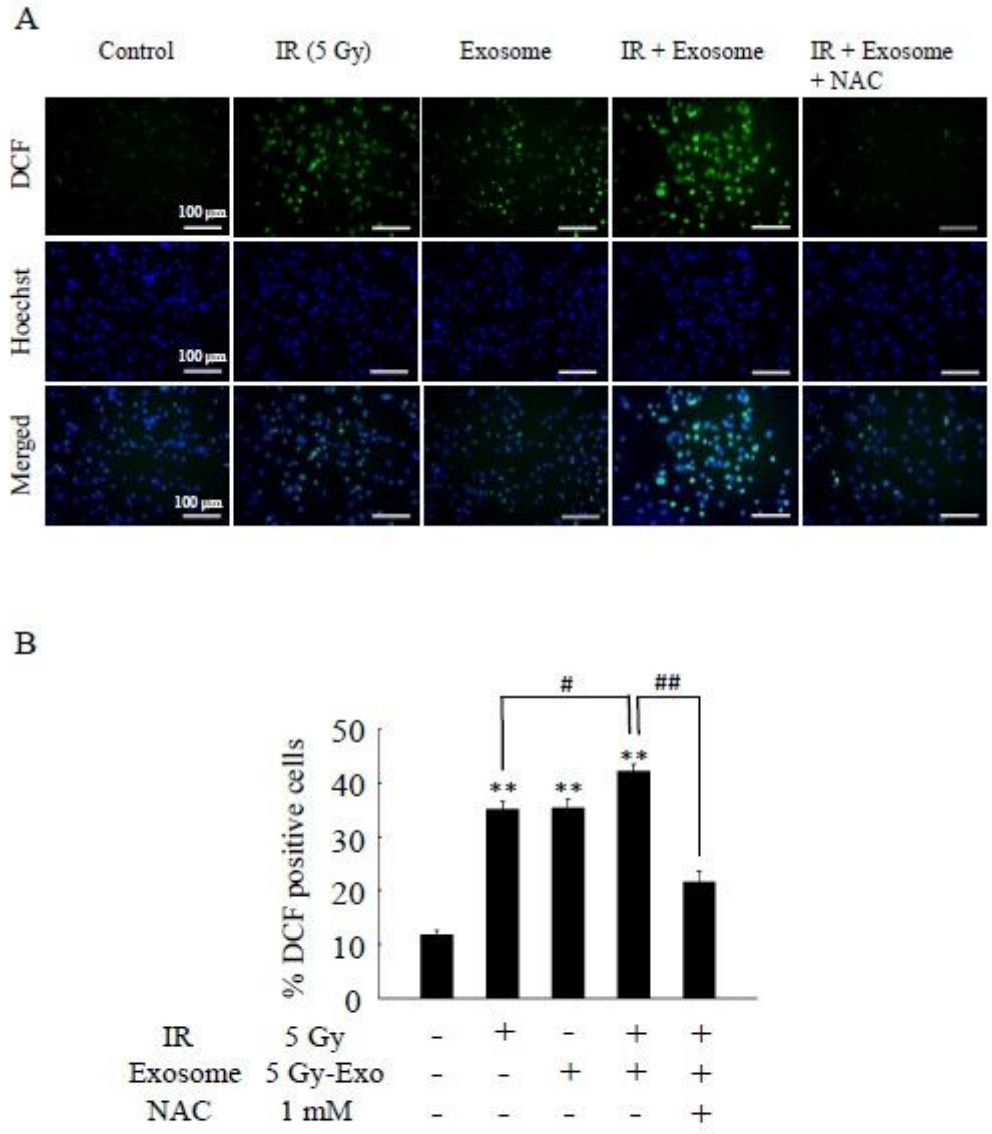

Figure 3

A) ROS-producing cells identified by C-H2DCF staining. B) The ratio of C-H2DCF positive cells. Proportions of DCF-positive cells were calculated mean ± SE from 3 fields for each section. P-value was calculated by using t-test. ** $P < 0.01$ compared with control; # $P < 0.05$, ## $P < 0.01$ compared with the IR + Exo group.

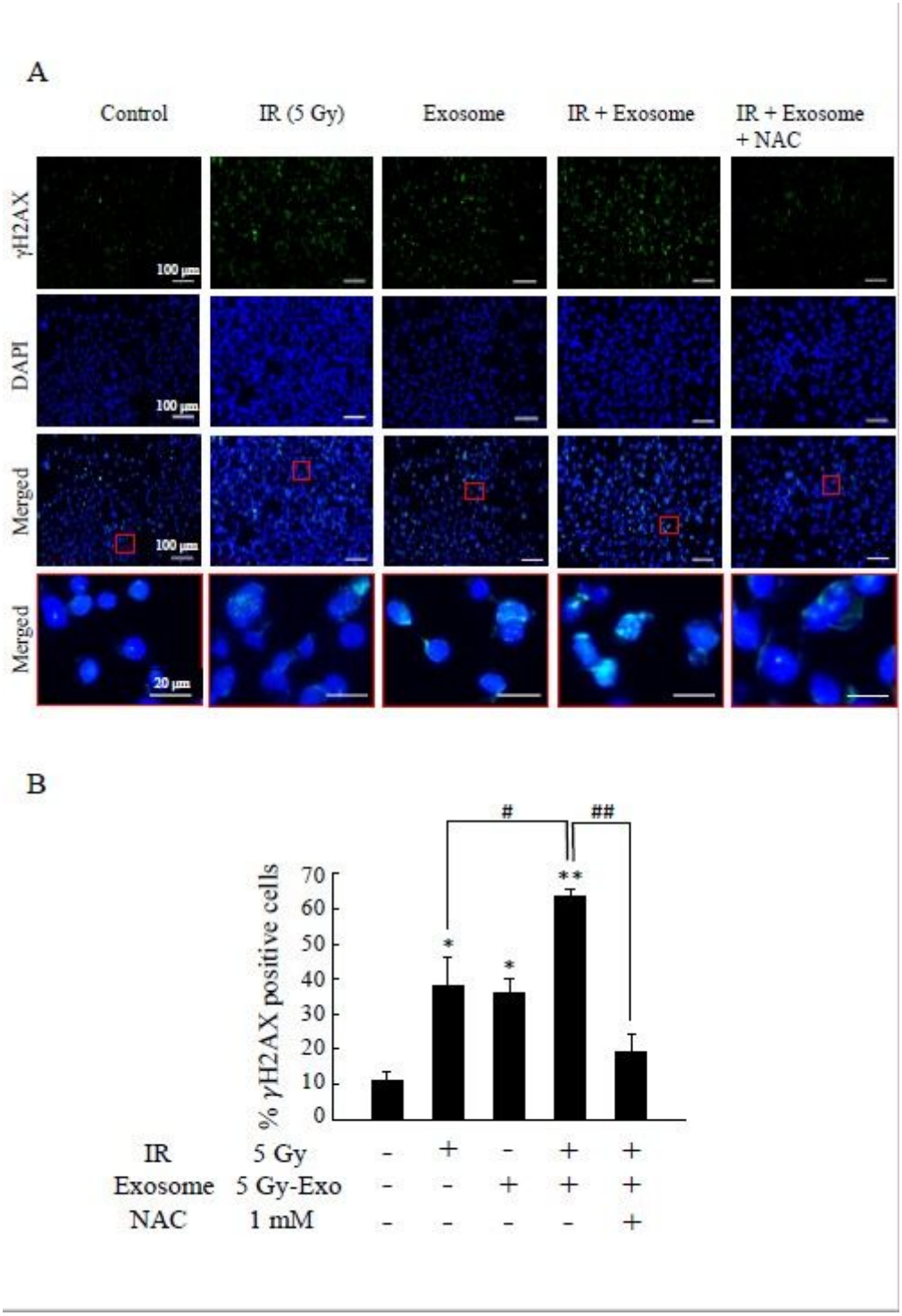

Figure 4

A) Representative images of cells with DNA damage identified by anti-γH2AX antibody (green) treatment and counterstaining with DAPI (blue). B) The proportion of γH2AX-positive cells was calculated as mean ± SE from 3 fields for each section. P value was calculated by using t-test. * $P < 0.05$, ** $P < 0.01$ compared with control; # $P < 0.05$, ## $P < 0.01$ compared with the IR + Exo group.

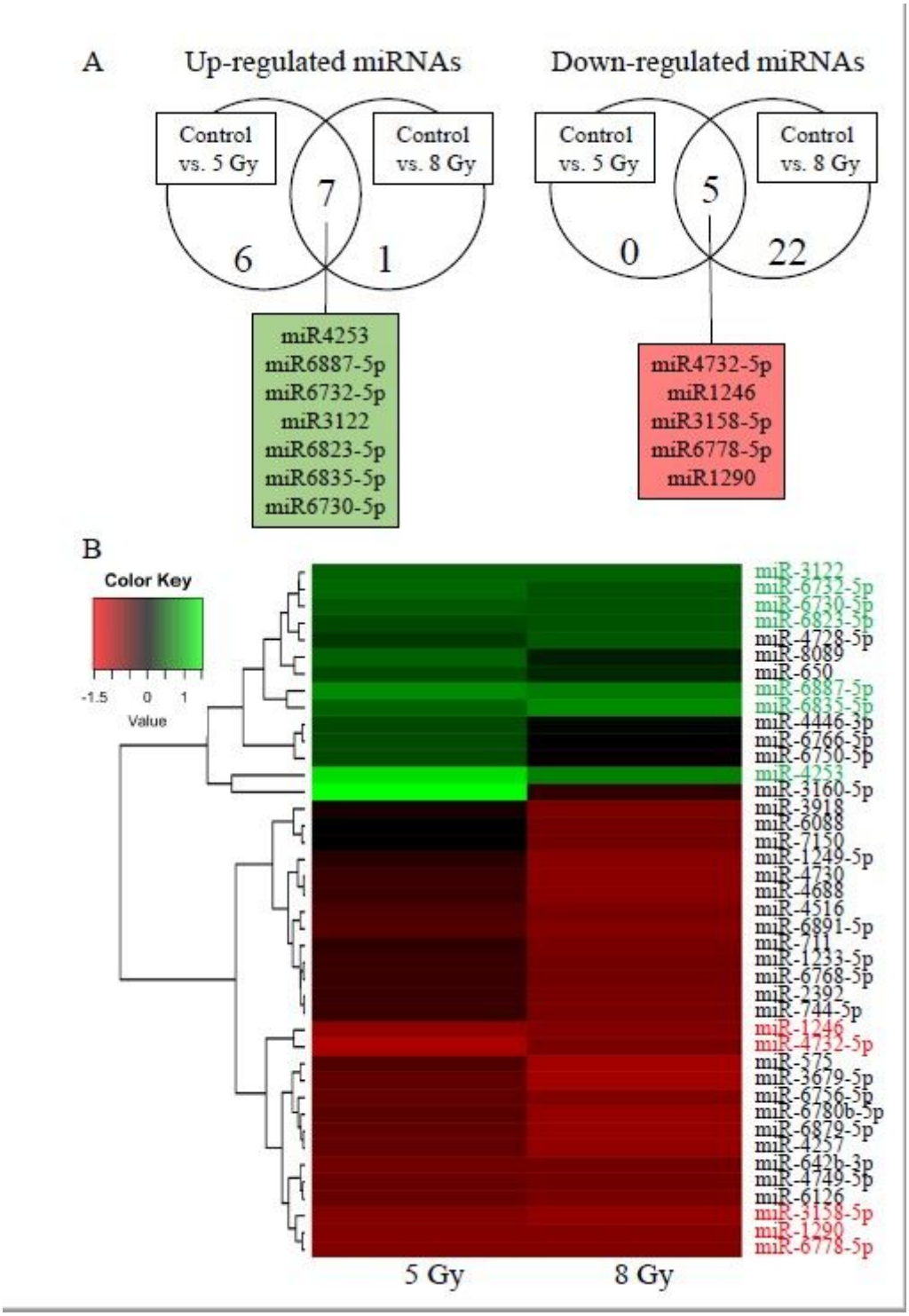

Figure 5

MiRNAs identified after 5 Gy-Exo and/or 8 Gy-Exo treatment. A) Venn diagram depicts the distribution of miRNAs in 5 Gy-Exo and 8 Gy-Exo samples. B) A heat map generated using the results.

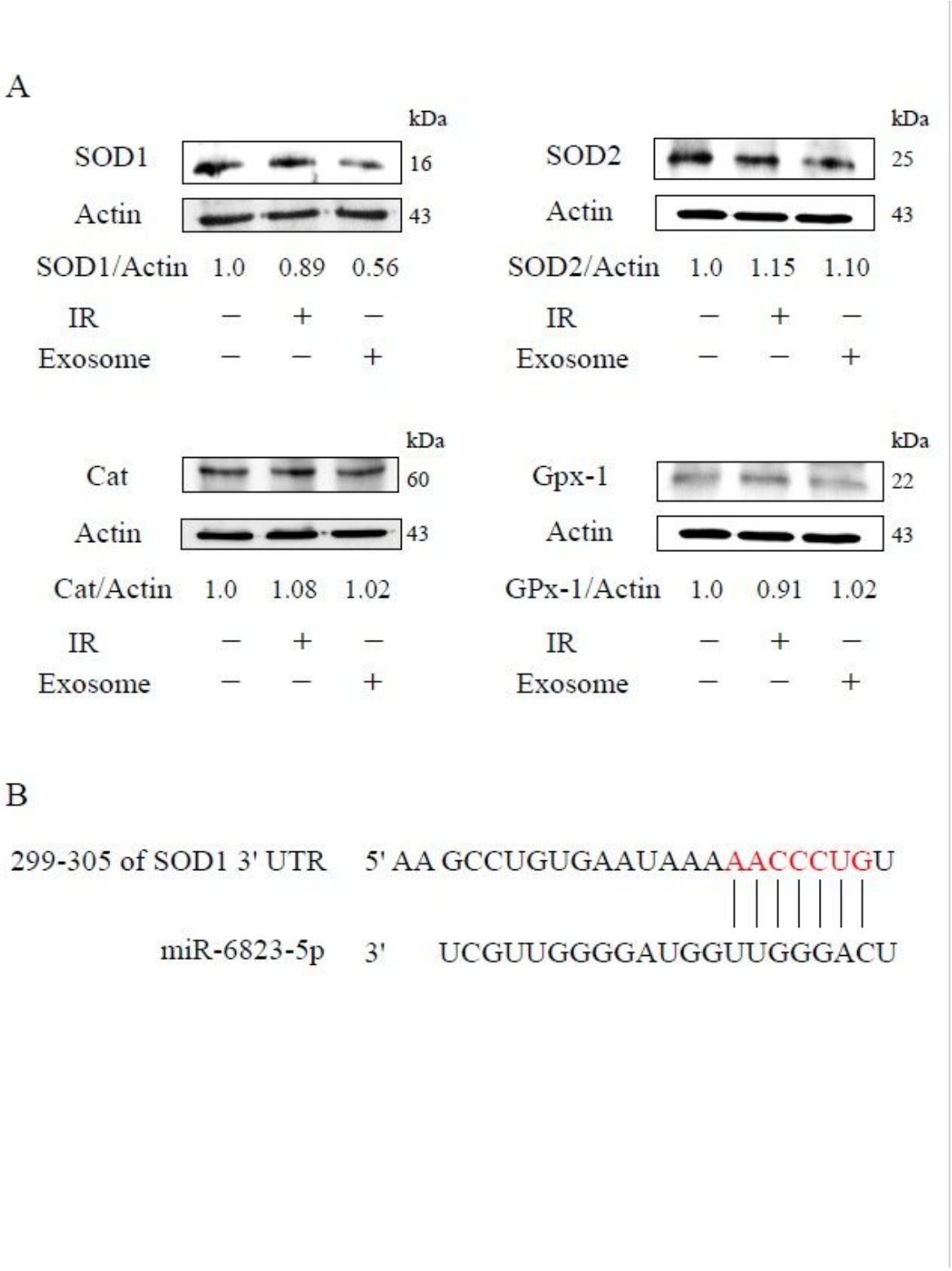

Figure 6

A) SOD1, SOD2, Catalase and GPX-1 expression after irradiation or exosome addition. B) Complementary sequence site of SOD1 and miR-6823-5p.

Supplementary Files

This is a list of supplementary files associated with this preprint. Click to download.

- 81896MIA20Gy20170219072742.mpg
- 81896MIA25Gy20170219065551.mpg